

# Droplet Collision Outcomes at High Weber Number

N. Roth<sup>1\*</sup>, C. Rabe<sup>2</sup>, B. Weigand<sup>1</sup>, F. Feuillebois<sup>3</sup>, J. Malet<sup>2</sup>

<sup>1</sup>Institut für Thermodynamik der Luft- und Raumfahrt (ITLR), Universität Stuttgart, Pfaffenwaldring 31, 70569 Stuttgart, Germany

<sup>2</sup>Institut de Radioprotection et de Sûreté Nucléaire (IRSN) DSU/SERAC Laboratoire d'Etudes et de Modélisation en Aérodispersion et Confinement BP68, 91192 Gif-sur-Yvette Cedex, France

<sup>3</sup>Laboratoire de Physique et Mécanique des Milieux Hétérogènes, - UMR CNRS 7636 Ecole Supérieure de Physique et de Chimie Industrielles, 10, rue Vauquelin 75231 Paris Cedex 05, FRANCE

## Abstract

Droplet collisions for Weber numbers from 500 up to 2600 have been studied. Experiments have been performed with water and iso-propanol for different impact parameters and different droplet sizes. For higher Weber numbers and in a range of the impact parameter larger than zero a new outcome regime has been observed with larger droplets than found for grazing impacts at impact parameters close to one. Differences for the two liquids and the droplet sizes studied have been identified.

## Introduction and objectives

During the course of a hypothetical severe accident in a Pressurized Water Reactor (PWR), hydrogen can be produced by the core oxidation and distributed into the whole containment. In order to assess the risk of detonation, spray systems can be put at the top of the containment to ensure a mixing of the atmosphere, to reduce the total pressure, to cool down the containment walls, and to wash-out the eventually existing fission products present in the air. Spray systems in reactor applications are composed of over 500 interacting water droplet sprays. Droplets are between 100 and 1000  $\mu\text{m}$  large, and are used under pressure (2-3 bars) at water temperatures between 20 and 60  $^{\circ}\text{C}$ , and under gaseous mixture composed of water steam, hydrogen and air at temperatures between 60 and 120  $^{\circ}\text{C}$  [1]. The droplet size distribution in the containment vessel could have an influence on the spray system efficiency. The droplet size evolution can be modelled by gravity and drag forces, heat and mass transfer with the surrounding gas, and droplets interactions. This paper will focus on this latter phenomenon, i.e. on droplet collision. In simulations of interacting sprays, the modeling of the collision process is absolutely necessary. In order to develop a realistic model of collision, the characteristic droplet size distributions are essential.

To simplify the problem, interaction has first to be studied between two drops as depicted in Fig. 1. Binary droplet collisions may result in different outcome regimes like bouncing, coagulation, reflexive separation or stretching separation [2]. These regimes depend on the collision geometry and on dimensionless parameters characterizing the liquid flow.

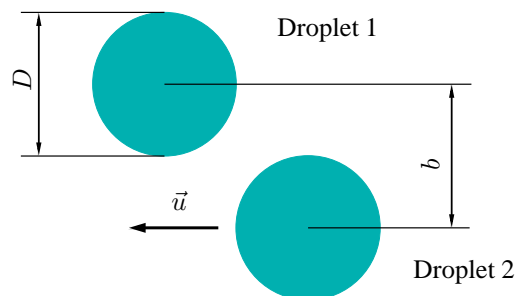


**Figure 1.** Schematical view of the collision of two equally sized droplets of diameter  $D$  and relative velocity  $u$ . The eccentricity of the collision is  $b$ .

All of the regimes mentioned above are observed for Weber numbers lower than 200. The objective of this paper is to investigate collision outcomes for a wider range

\*Corresponding Author: norbert.roth@itlr.uni-stuttgart.de  
Proceedings of the 21<sup>st</sup> ILASS - Europe Meeting 2007

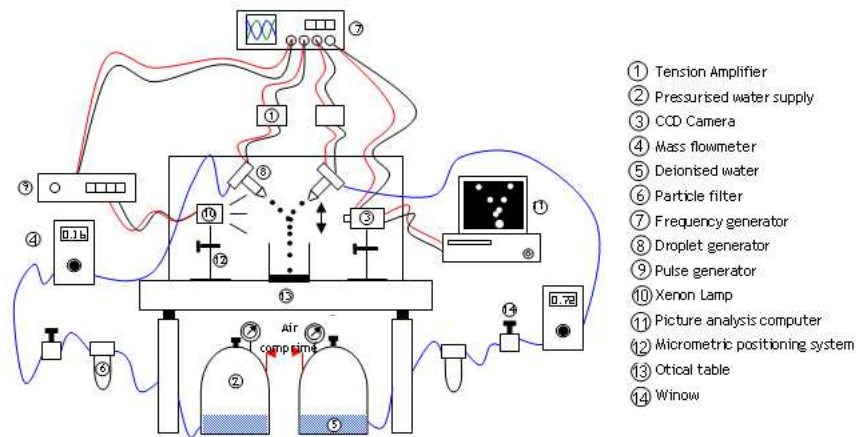


**Figure 2.** IRSN experimental set-up for water droplet coalescence studies.

of Weber numbers that can be found in various applications (e. g. in sprays used in nuclear containments, the Weber number can vary from 10 to 3000). Droplet collisions at Weber numbers higher than 1000 may result in splashing [3] for head-on collisions with the dimensionless eccentricity  $B = b/D = 0$ , where  $b$  is the eccentricity and  $D$  the droplet diameter (compare Fig. 1 or [2]). In this study, two similar experimental setups have been used in order to investigate the collision processes under higher Weber number. One setup has been used to work on iso-propanol droplets (ITLR setup) and the other one has been used to investigate water droplet interaction (IRSN setup).

### Experimental setup

In the experiments, two monodisperse and coherent droplet streams are used, produced by independent droplet stream generators developed by ITLR [3].

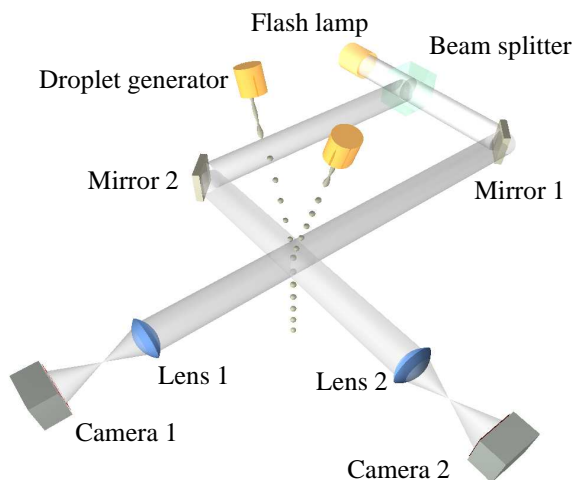


**Figure 3.** ITLR experimental set-up for iso-propanol droplet coalescence studies. Two views perpendicular to each other can be recorded.

The first set of experiments was performed at ITLR with iso-propanol of density  $\rho = 801.6 \text{ kg/m}^3$ , surface tension  $\sigma = 2.17 \cdot 10^{-2} \text{ N/m}$ , and dynamic viscosity  $\mu = 2.3 \cdot 10^{-3} \text{ kg/(m} \cdot \text{s)}$ . The second set of experiments was conducted at the IRSN where a similar setup had been built (Fig. 2), to investigate, in the same way, high Weber number collisions for pure water droplet of  $\rho = 998.2 \text{ kg/m}^3$ ,  $\sigma = 7.28 \cdot 10^{-2} \text{ N/m}$ , and  $\mu = 1.0 \cdot 10^{-3} \text{ kg/(m} \cdot \text{s)}$ . A semi-automatic image processing for the water droplet collisions study allows an important number of measurements.

In the ITLR setup, two independent views of the collision process from different directions is recorded at the same time, as can be seen from Fig. 3. These views are perpendicular to each other, one showing the plane of the droplet trajectories. From the records, the limits of the different regimes can be identified and the development of the collision process can be evaluated at least for head-on collisions. In the IRSN setup, only one view is recorded at one time.

### Results and Discussion

#### *New collision outcomes*

Experimental results have been obtained for different values of the Weber number. A collision process of iso-propanol droplets for a high Weber number is shown in Fig. 4 and for water droplets in Fig. 5. The individual droplets are moving from top to bottom, thus the collision process advances from top to bottom. Results are shown for different eccentricities. With a high eccentricity ( $B = 0.45$  for iso-propanol and  $B = 0.92$  for water) *stretching separation* can be observed with two large droplets and a lot of tiny droplets deriving from Rayleigh disintegration of the thin filament. For intermediate eccentricities ( $B = 0.36$  for iso-propanol and  $B = 0.54$  for water) a new regime can be identified with the stretching of a disk resulting first in a filament, while fingers perpendicular to the filament can be observed. The rather thick

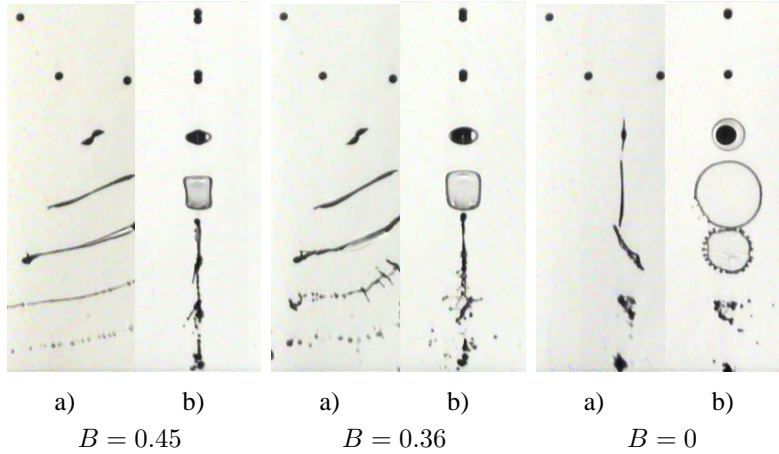


**Figure 4.** Photographs of two colliding iso-propanol droplet streams for  $We = \rho Du^2/\sigma = 1824$ , Reynolds number  $Re = \rho Du/\mu = 1050$ , droplet diameter,  $D = 184 \mu\text{m}$ , relative droplet velocity  $u = 16.4 \text{ m/s}$  and size ratio between the colliding droplets of 1.

a) view in the plane of the trajectories.  
b) view in the perpendicular plane.

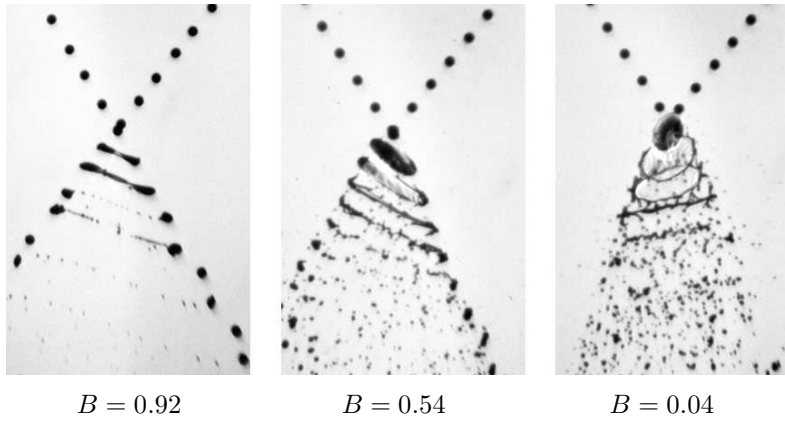


**Figure 5.** Photographs of two colliding water droplet streams for  $We = 1849$ , Reynolds number  $Re = 5424$ , droplet diameter  $D = 220 \mu\text{m}$ , relative droplet velocity  $u = 24.5 \text{ m/s}$  and size ratio between the colliding droplets of 1.

filament disintegrates into larger droplets and the fingers form tiny droplets (*stretching with fingers*). On the right hand side, the corresponding head-on collision ( $B \simeq 0$ ), which results in splashing, can be seen.

#### Detailed results for $B = 0$

The colliding droplets form a Saturn-like object for very early phases of the impact, which is transformed into a circular disk with large diameter. The rim of the disk shows instabilities, which form first nodes, then fingers and finally, if the Weber number is higher, many tiny droplets. This process of development of a disk with fingers is quantified in Fig. 6 for iso-propanol droplets, the disk diameter and the length of the fingers are shown as a function of time  $t^* = tu/D$  in a dimensionless presentation for  $We = 1824$  and for  $B = 0$ . It can be seen that no significant fingers are found before the disk has reached its maximum value. At  $We = 1824$ , the ratio between the length and thickness of the fingers is still too small to allow the formation of tiny droplets around the disk due to Rayleigh instabilities. The limit of the Weber number for the formation of such tiny droplets is important, because this may change the heat and mass transfer behavior significantly.

#### Detailed results for $B \neq 0$

As stated above, for intermediate eccentricities a transition outcome between *splashing* and *stretching* separation called *stretching with fingers* or *stretching with digitations* can be observed (see Fig. 7-a). This kind of outcome starts by an ellipsis development, which grows in the direction of the relative velocity between the two droplets, and collapse in a filament, after a little time, because of a kinetic energy lack. As for *splashing* separation, Rayleigh instabilities lead to nodes creation along this filament which form the basis of fingers. In this case, fingers and filament parts between nodes result in small satellite droplets as nodes disintegrate in larger ones. For this reason, *stretching with fingers* allows larger satellite droplets production, that means larger than in the case of simple *stretching* (see Fig. 7-b). Deeper analysis of these regimes has been performed with water droplet collisions. Thanks to the IRSN semi-automatic device for water droplet collision characterisation, the transition occurrence between various outcomes has been observed and plotted on Fig. 8. On the left part of the graph, collisions with  $We < 500$  correspond to *reflexion* and *stretching*

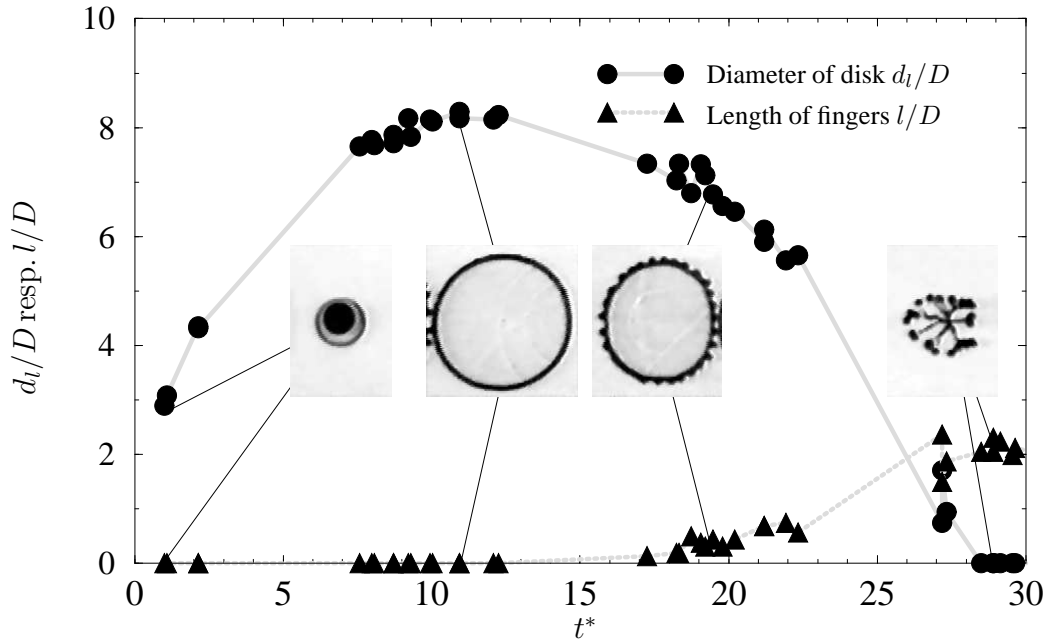


**Figure 6.** Diameter of the liquid disk and length of the fingers as a function of time for iso-propanol droplet collisions. In this dimensionless presentation, the circles indicate  $d_i/D$  ( $d_i$  : disk diameter) and the triangles  $l/D$  ( $l$  : finger length). The shape of the disk with fingers is shown at four different times. The Weber number was  $We = 1824$ .

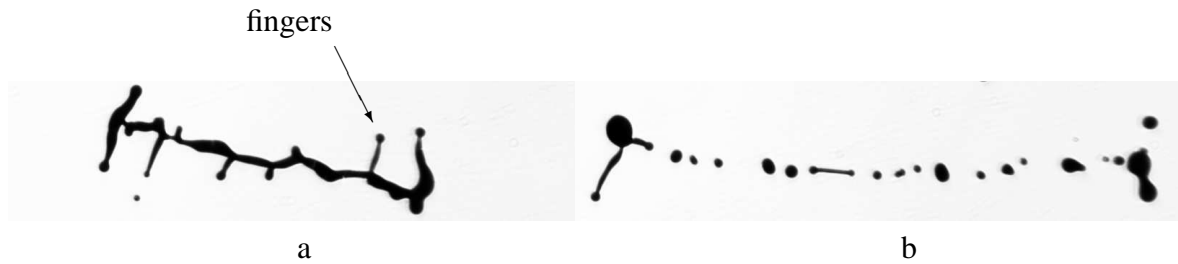


**Figure 7.** Enlarged view of the disintegration process with fingers that can be observed in picture (a) and finally resulting in larger droplets to be observed in picture (b).

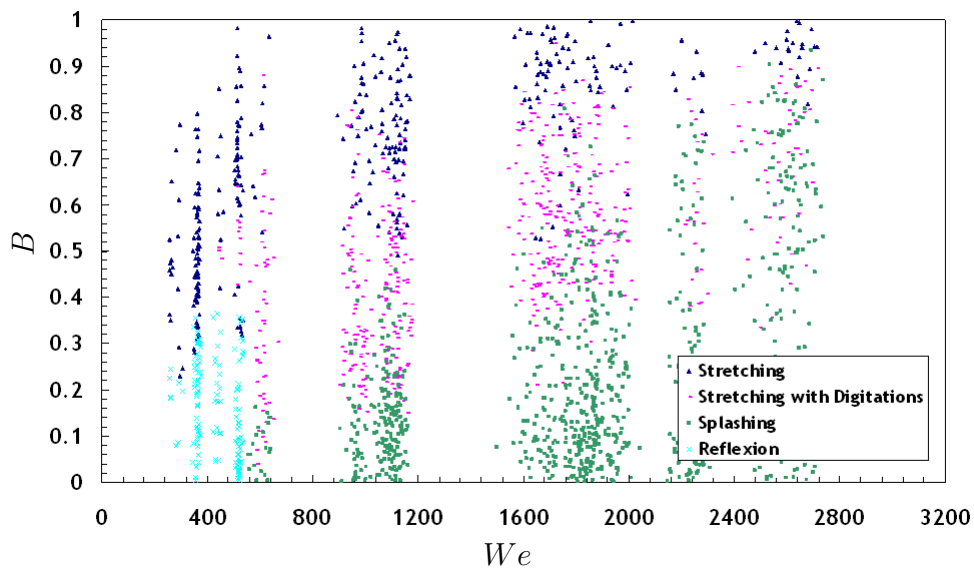


**Figure 8.** Results obtained on the IRSN set-up for water droplet collisions. Droplet size is  $220 \mu\text{m}$  and the size ratio is 1.

outcomes. This collision outcomes had generally been described in the literature (see [4]) for  $We < 200$ . Our results show that their eccentricity boundary limit takes place between 0.3 and 0.4, which is in good agreement with *Ashgriz and Poo's* theory. A whole description of the mechanisms governing these regimes could be found in [5]. On the right part of Fig. 8, the new regimes, identified previously in this paper, clearly appear. Few characteristics of their transition fields could be pointed out:

- For  $We > 500$ , *reflexion* is replaced by *splashing* and *stretching with fingers* as *stretching* separation keeps also important.
- At  $We \approx 500$ , the limit between *splashing* / *stretching with fingers* is located between 0.05 and 0.15, due to a high energy present in head-on collisions, necessary for fingers enlargement. As a consequence, the maximum eccentricity which allows *splashing*, increases with the Weber number to reach 0.7 for  $We \approx 2600$ .
- The limit between *stretching with fingers* and *reflexion*, needs some further investigation to be well defined.
- Transition between *stretching with fingers* and *stretching*, at  $We \approx 500$ , occurs for an eccentricity  $B$  between 0.55 and 0.65.
- It can be seen on the graph that *stretching with fingers* field, quite large very early, grows with the Weber number, before being replaced by *splashing*.
- For higher  $We (> 2000)$ , a large impact parameter domain is covered by *splashing*, as *stretching* takes only place for the most grazing collisions.

According to our results, at high Weber numbers, the droplets have excess kinetic energy, which leads to a quick separation in many satellite droplets in order to redistribute the total energy, directly after collision.

#### *Investigation of other influencing parameters on collisions at Weber number higher than 200*

Earlier studies on droplet collisions (see [2]) have shown that the collisional dynamics of droplets for various liquids could significantly be different. Diagrams showing

that the eccentricity  $B$  as a function of the Weber number  $We$  is not universal and can be dependent of other parameters that are not yet well defined. In this study, parameters which have been investigated qualitatively are the liquid nature, the droplet size, and the collision angle. Despite the fact that the two liquids studied have different physical properties, we produce at first droplets of the same diameter and with the same  $We$  during collision. Then, the droplets diameter was changed on one part and the collision angle on the other.

Results are summarized in Table 1. In this table, Bc1 represents the boundary condition (eccentricity  $B$ ) between *splashing* and *stretching with fingers*, as Bc2 represents the same condition between *stretching with fingers* and *stretching*.

Further observations have been made concerning the results reported in this table:

- Droplet fluid: results for water and iso-propanol droplets of approximately the same diameter and same Weber number show a large difference between eccentricities transition values. As both transitions outcomes for water droplets are higher, the assumption that iso-propanol droplets dissipate more kinetic energy than water droplets, during the collision, could be formulated.
- Droplet size: a droplet size of  $450 \mu\text{m}$  has been investigated with water droplets and shows huge differences with smaller droplets of  $220 \mu\text{m}$ . If transition between *reflexion* and new collision outcomes seem to take also place at  $We \approx 500$ , the *splashing* regime overcomes the other ones faster than for smaller droplet sizes. Actually, at  $We \approx 1000$ , collisions for this droplet size lead almost only to *splashing*.
- Collision angle: results obtained for iso-propanol droplets with different collision angles give no significant disparity to be taken into account like other influent parameters.

Table 1 shows that the boundary between the new collision outcomes depend not only on eccentricity  $B$  and Weber number  $We$ , but also on liquid properties and droplet volume which had ever been pointed out for other collision outcomes (coalescence, reflexion, bouncing and stretching) in a small range of Weber Number

Fluid	Water	Water	Iso-propanol	Iso-propanol
Droplet diameter ( $\mu\text{m}$ )	220	450	252	255
Collision angle ( $^\circ$ )	69.1	109.4	56.7	76.6
Weber number	1034	1053	1038	1035
Reynolds number	4193	5617	888	892
Bc1	0.15 to 0.3	only <i>splashing</i>	0.05 to 0.2	0.05 to 0.2
Bc2	0.55 to 0.75	only <i>splashing</i>	0.4 to 0.6	0.4 to 0.6

**Table 1.** Experimental values for transition eccentricities between collision outcomes, depending on fluid properties, droplets diameter and collision angle.

( $We \approx 200$ ). Moreover the influence of collision angle has not been demonstrated and seems not to be important. Nevertheless, the Reynolds number evolution is in accordance with the one of the various transition values and might be used to characterise them with a better accuracy.

### Conclusion

Current models for the outcomes of binary droplet collision, for hydrocarbon or water droplets, are limited to Weber numbers lower than 200. The results of the present investigation will help for establishing semi-empirical correlations describing the droplet size evolution in a spray due to coalescence processes in a wider range of Weber number than established previously. A detailed description of new collision events was given thanks to large series of pictures with various collision angles, droplet diameters, and using two different liquids: isopropanol and water. Actually, new experimental results have shown, for  $We > 500$ , the occurrence of two new regimes, *splashing* and *stretching with fingers*, which have never been studied before. Behaviour and time evolution of colliding droplets during such outcomes have been explained in order to understand their governing mechanisms.

Additionally, an almost complete series of data for 220  $\mu\text{m}$  water droplet collisions, depending on Weber number and excentricity, have been reported and used to describe the transition between these new regimes. So, boundary conditions for the outcomes have been plotted and their evolution clearly pointed out. Furthermore, comparisons were made to demonstrate that the eccen-

tricity values of these transitions are linked to the liquid properties at first, and also to the droplet size, whereas collision angle seems to have no significant direct influence on it.

Finally, Reynolds number calculation, for various collision conditions, suggests that it would be a suitable parameter for droplet collision behaviour for high Weber number.

### References

- [1] **Plumecocq W.**, *Etude de l'interaction d'un système d'aspersion liquide avec l'atmosphère environnante*, PhD thesis, Université de provence (Aix-Marseille I), 1997.
- [2] **Qian J. & Law C.K.**, *Regimes of coalescence and separation in droplet collisions*, J. Fluid Mech., 331, 59–80, 1997.
- [3] **Roth N., Rieber M. & Frohn A.**, *High energy head-on collisions of droplets*, In Proc. 15th Int. Conf. on Liquid Atomization and Spray Systems, Toulouse, France, 1999. ILASS.
- [4] **Estrade J. P., Carentz H., Lavergne G. & Biscos Y.**, *Experimental investigation of dynamic binary collision of ethanol droplet - model for droplet coalescence and bouncing*, In Proc. 14th Int. Conference on Liquid Atomization and Spray Systems, 528–533, 1998.
- [5] **Ashgriz N. & Poo J.Y.**, *Coalescence and separation in binary collisions of liquid drops*, J. Fluid Mech., 221, 183–204, 1990.